Cellular and Molecular Life Sciences (2023) 80:120
https://doi.org/10.1007/s00018-023-04767-y

ORIGINAL ARTICLE

HIF-1α-activated TMEM237 promotes hepatocellular carcinoma progression via the NPHP1/Pyk2/ERK pathway

Tianxiang Chen[1] · Liang Wang[2] · Chao Chen[3] · Runtian Li[1] · Ning Zhu[4] · Runkun Liu[1] · Yongshen Niu[1] · Zhengtao Xiao[5] · Hui Liu[6] · Qingguang Liu[1] · Kangsheng Tu[1]

Received: 22 December 2022 / Revised: 21 March 2023 / Accepted: 22 March 2023 / Published online: 11 April 2023

Abstract

Background Hypoxia-inducible factors (HIFs) are the most essential endogenous transcription factors in the hypoxic microenvironment and regulate multiple genes involved in the proliferation, migration, invasion, and EMT of hepatocellular carcinoma (HCC) cells. However, the regulatory mechanism of HIFs in driving HCC progression remains poorly understood.

Methods Gain- and loss-of-function experiments were carried out to investigate the role of TMEM237 in vitro and in vivo. The molecular mechanisms involved in HIF-1α-induced TMEM237 expression and TMEM237-mediated enhancement of HCC progression were confirmed by luciferase reporter, ChIP, IP-MS and Co-IP assays.

Results TMEM237 was identified as a novel hypoxia-responsive gene in HCC. HIF-1α directly bound to the promoter of TMEM237 to transactivate its expression. The overexpression of TMEM237 was frequently detected in HCC and associated with poor clinical outcomes in patients. TMEM237 facilitated the proliferation, migration, invasion, and EMT of HCC cells and promoted tumor growth and metastasis in mice. TMEM237 interacted with NPHP1 and strengthened the interaction between NPHP1 and Pyk2 to trigger the phosphorylation of Pyk2 and ERK1/2, thereby contributing to HCC progression. The TMEM237/NPHP1 axis mediates hypoxia-induced activation of the Pyk2/ERK1/2 pathway in HCC cells.

Conclusions Our study demonstrated that HIF-1α-activated TMEM237 interacted with NPHP1 to activate the Pyk2/ERK pathway, thereby promoting HCC progression.

Keywords Hypoxia · Hepatocellular carcinoma · TMEM237 · NPHP1 · Pyk2/ERK pathway

Tianxiang Chen and Liang Wang contributed equally to this work.

✉ Qingguang Liu
liuqingguang@vip.sina.com

✉ Kangsheng Tu
tks0912@foxmail.com

[1] Department of Hepatobiliary Surgery, The First Affiliated Hospital of Xi'an Jiaotong University, Xi'an 710061, China

[2] Department of Burn and Plastic Surgery, Shaanxi Provincial People's Hospital, Xi'an 710068, China

[3] Department of General Surgery, The First Affiliated Hospital of Xi'an Medical University, Xi'an 710077, China

[4] The Key Laboratory of Tumor Molecular Diagnosis and Individualized Medicine of Zhejiang Province, Zhejiang Provincial People's Hospital, Affiliated People's Hospital, Hangzhou Medical College, Hangzhou 310014, China

[5] Department of Biochemistry and Molecular Biology, School of Basic Medical Science, Xi'an Jiaotong University Health Science Center, Xi'an 710061, China

[6] Department of Medical Equipment, Shaanxi Provincial People's Hospital, Xi'an 710068, China

Abbreviations

HCC	Hepatocellular carcinoma
HIFs	Hypoxia-inducible factors
PHD	Prolyl hydroxylase
HREs	Hypoxia-responsive elements
TMEM237	Transmembrane protein 237
JSRDs	Joubert syndrome-related disorders
EMT	Epithelial–mesenchymal transition

Introduction

Hepatocellular carcinoma (HCC) is one of the most common malignancies, accounting for approximately 830,000 deaths annually [1]. Although large efforts have been made in diagnosis and therapy in recent decades, the treatment effect of HCC is still unsatisfactory [2]. Due to the insidious onset and rapid progression of HCC, many patients are diagnosed in the middle or late stages, losing the opportunity to undergo radical treatment [3]. Therefore, it is

imperative to identify more effective diagnostic and therapeutic approaches for HCC.

Extensive studies have reported that hypoxia, which occurs ubiquitously in solid tumors, plays an essential role in the progression of malignancy [4]. Hypoxia-inducible factors (HIFs), a hallmark of hypoxia, are heterodimers comprising the HIF-1/2α subunit and HIF-1β subunit [5]. The HIF-1/2α subunit, which is hydroxylated by prolyl hydroxylase (PHD) and degraded by the ubiquitin−proteasome pathway under normoxic conditions, accumulates and forms a complex with HIF-1β under hypoxic conditions to regulate the transcription of target genes by binding to hypoxia-responsive elements (HREs) in the promoter [5]. Accumulating evidence has demonstrated that hypoxia exerts multidimensional effects on HCC growth, metastasis, angiogenesis, metabolism reprogramming, stemness properties and immune evasion [6]. Our previous studies revealed that hypoxia-responsive genes, including cofilin 1 [7], peptidyl arginine deiminase 4 [8], RUNX1-IT1 [9], KDM4A-AS1 [10] and MAPKAPK5-AS1 [11], are involved in HCC growth, metastasis and vascularization. However, more investigations should be conducted to unravel the role of hypoxia in HCC.

Membrane proteins account for 20–30% of all human proteins, exerting pleiotropic biological functions as receptors, enzymes, anchorage proteins or structural proteins [12, 13]. The structure and function of most membrane proteins are clearly delineated, while many transmembrane proteins, which are classified into the transmembrane protein (TMEM) family, are still poorly understood [13, 14]. Emerging studies have shown that TMEMs are dysregulated and act as oncogenes or tumor suppressors in various types of cancer, such as colorectal cancer [15], ovarian cancer [16], lung cancer [17], breast cancer [18] and HCC [19, 20]. Based on our previous microarray data (GSE155505) [11], we found that TMEM237 was upregulated under hypoxic conditions in Hep3B cells. TMEM237, also known as ALS2CR4 or JBTS14, may be involved in membrane trafficking between the inner and outer segments of retinal photoreceptors [21]. Additionally, TMEM237 is mutated in individuals with disorders associated with Joubert syndrome [22]. TCGA data analysis indicated that high TMEM237 levels predicted a poor prognosis in HCC patients. However, the biological function and molecular mechanism of TMEM237 in HCC remain largely elusive.

In this study, we unraveled the regulatory mechanisms involved in the effects of hypoxia on TMEM237 expression. Furthermore, we investigated the expression, clinical significance, and biological function of TMEM237 and explored the mechanisms underlying the role of TMEM237 in HCC. This study revealed novel insights into the role of hypoxia in HCC and suggested TMEM237 as a promising therapeutic target for HCC.

Materials and methods

Patients and clinical specimens

Ninety pairs of HCC and adjacent nontumor tissues from patients undergoing hepatectomy at the First Affiliated Hospital of Xi'an Jiaotong University (Xi'an, China) were snap frozen in liquid nitrogen and stored at − 80 °C or 10% formalin-fixed and paraffin-embedded. All patients included in this study were pathologically diagnosed with HCC and received no preoperative anticancer therapy. The clinicopathological and demographic information of the patients is described in Table 1. All procedures involving human participants were in compliance with the ethical standards of the Research Ethics Committee of The First Affiliated Hospital of Xi'an Jiaotong University and with the Declaration of Helsinki revised in 2013 (XJTU1AF2020LSY-08). Written informed consent for HCC patients to participate in the study was obtained before sample collection.

Cell culture

Human HCC cell lines (Hep3B, Huh7, PLC/PRF/5, HepG2, MHCC97L, MHCC97H, and HCCLM3), the immortalized normal hepatic cell line MIHA, and HEK293T cells were maintained in our lab [23]. All cells were cultured in Dulbecco's modified Eagle's medium (DMEM; Gibco; Thermo Fisher Scientific, Inc., Waltham, MA, USA) supplemented with 10% fetal bovine serum (FBS; Gibco; Thermo Fisher Scientific, Inc.) and 1% penicillin−streptomycin (Gibco; Thermo Fisher Scientific, Inc.) in a humidified 5% CO_2 incubator at 37 °C. Hypoxic conditions were established with a multigas incubator obtained from PHC Holdings Corporation (Tokyo, Japan).

Lentivirus transduction

TMEM237 shRNAs (shTMEM237#1, shTMEM237#2 and shTMEM237#3) and scrambled shRNA (shNC) were designed and synthesized by GeneCopoeia, Inc. (Guangzhou, China). NPHP1 shRNA (shNPHP1) and scrambled shRNA (shNC) were obtained from Tsingke Biotechnology Co., Ltd. (Beijing, China). The human TMEM237 ORF cDNA clone (TMEM237), the human NPHP1 ORF cDNA clone (NPHP1) and control empty vector (EV) were purchased from GeneCopoeia, Inc. HIF-1α shRNA (shHIF-1α), HIF-2α shRNA (shHIF-2α) and scrambled shRNA (shNC) were purchased from GeneCopoeia, Inc. For lentiviral production, the target plasmids were transfected into HEK293T cells along with psPAX2 packaging plasmid and pMD2.G envelope plasmid. Viral supernatant was collected and

Table 1 Clinical correlation of TMEM237 expression in HCC

Clinical parameters	Cases (n)	TMEM237 expression		P value
		High (n = 45)	Low (n = 45)	
Age				0.284
< 50 years	37	16	21	
≥ 50 years	53	29	24	
Gender				0.764
Male	77	38	39	
Female	13	7	6	
Tumor size				0.011*
< 5 cm	48	18	30	
≥ 5 cm	42	27	15	
Tumor number				0.042*
1	61	26	35	
≥ 2	29	19	10	
TNM stage				0.005**
I + II	70	29	41	
III + IV	20	16	4	
Edmondson–Steiner grading				0.153
I + II	66	30	36	
III + IV	24	15	9	
Venous infiltration				0.003**
Absent	54	20	34	
Present	36	25	11	
AFP				0.091
< 20 ng/ml	23	8	15	
≥ 20 ng/ml	67	37	30	
HBV infection				0.624
Absent	22	12	10	
Present	68	33	35	

TNM tumour-node-metastasis, *AFP* alpha-fetoprotein, *HBV* hepatitis B virus

*P < 0.05, **P < 0.01

filtered (0.45-μm pore size) after 48 h and then added to HCC cells with 8 μg/ml polybrene (Beyotime Biotech Inc., Shanghai, China). The shRNA sequences used in this study are shown in Supplementary Table 1.

RNA extraction and reverse transcription-quantitative polymerase chain reaction (RT-qPCR)

Tissues and cells were subjected to RNA extraction using RNAfast200 (Fastgen Biology Co., Ltd., Shanghai, China) according to the manufacturer's instructions, followed by cDNA synthesis using a cDNA Synthesis kit (Thermo Fisher Scientific, Inc.). RT−qPCR was performed with SYBR® Green Premix PCR Master Mix (Roche Diagnostics, Indianapolis, IN, USA). The primer sequences for TMEM237 were 5′-AGAGCACCATGAGGACTGAC (forward) and 5′-AGTTGATGGCTCATTGCCCT (reverse). The primer sequences for β-actin were 5′-ACTCGTCATACTCCTGCT (forward) and 5′-GAAACTACCTTCAACTCC (reverse).

Immunohistochemistry (IHC) staining

IHC was performed as previously described [10]. Briefly, paraffin-embedded sections were subjected to dewaxing, hydration and heat-induced antigen retrieval. Then, the primary antibodies were added to the sections and incubated at 4 °C overnight, followed by incubation with the corresponding secondary antibody (ZSGB-BIO, Inc.) at room temperature for 10 min. The slides were counterstained with hematoxylin and inspected under a microscope. The staining intensity score was evaluated on a scale of 0 (negative), 1 (weak), 2 (medium) or 3 (strong). The percentage score was defined as 0 (negative), 1 (1–25%), 2 (26–50%), 3 (51–75%) or 4 (76–100%). The IHC scores were obtained by multiplying the staining intensity score and the percentage score.

Western blotting and immunoprecipitation (IP) assays

Proteins from HCC cells and tissues were extracted using RIPA buffer (Beyotime Biotech Inc.) supplemented with proteinase inhibitors and phosphatase inhibitors. A BCA Protein assay kit (ZHHC Biotech Inc., Shaanxi, China) was used to determine the protein concentration according to the manufacturer's instructions. The lysates were separated by SDS–polyacrylamide gel electrophoresis and blotted onto polyvinylidene difluoride membranes. Then, the membranes were blocked with 10% nonfat milk and probed using primary antibodies at 4 °C overnight and the corresponding secondary antibodies at room temperature for 1 h. Finally, ECL reagent (Millipore, Merck Co., Ltd., Darmstadt, Germany) was used for signal detection. For the IP assay, the antibody or IgG (2 μg) was incubated with protein A/G magnetic beads (Thermo Fisher Scientific, Inc.) for 15 min at room temperature and then incubated with equal amounts of cell lysates (500 μg) at 4 °C overnight, and the immunoprecipitates were subjected to Western blotting. The antibodies used are listed in Supplementary Table 2.

Cell proliferation assay

CCK-8, colony formation, and EdU assays were conducted to examine the viability and proliferation of HCC cells. These assays were conducted as reported previously [23].

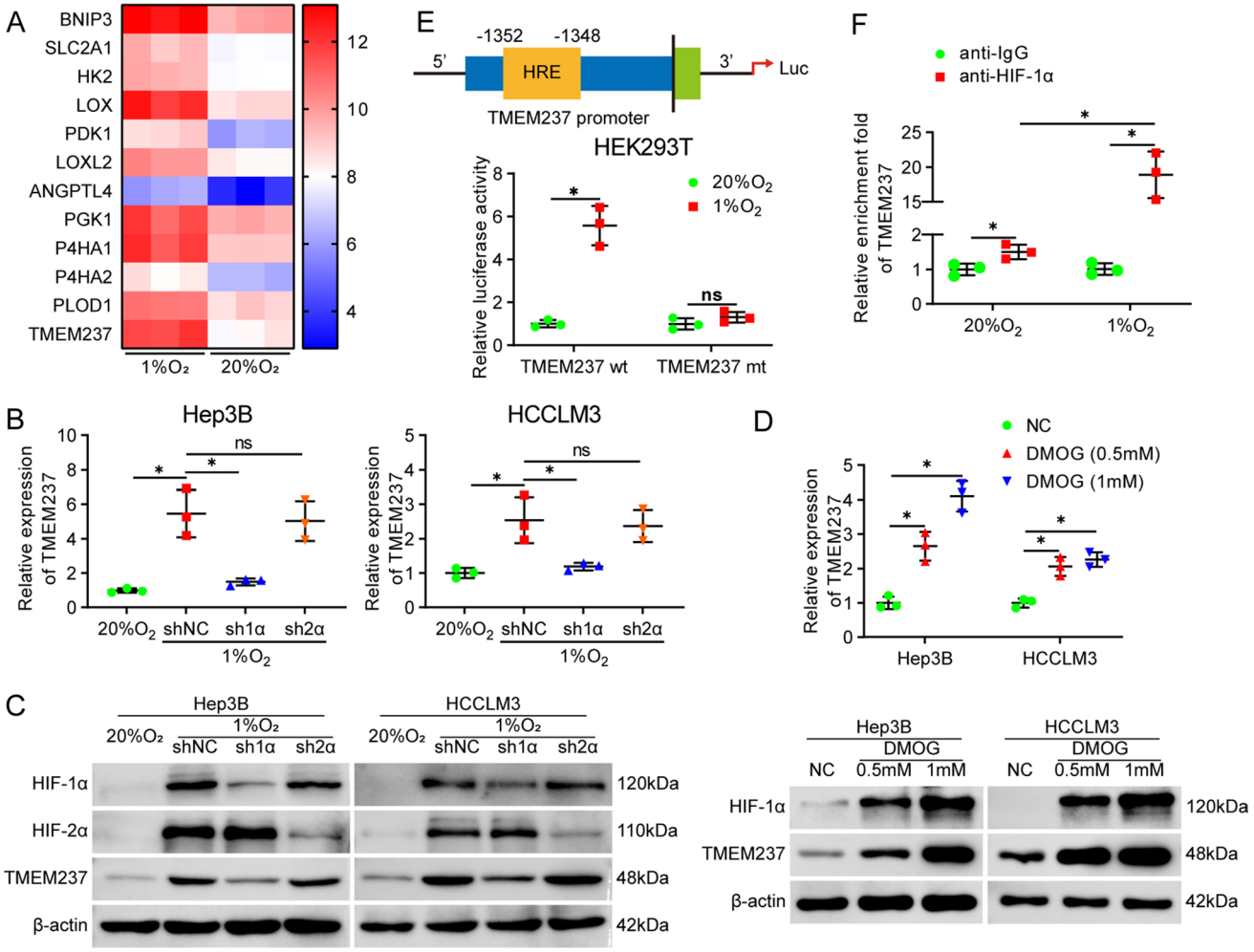

Fig. 1 Hypoxia upregulates TMEM237 expression via HIF-1α in HCC cells. **a** Heatmap of selected genes in Hep3B cells cultured under normoxic (20% O_2) or hypoxic (1% O_2) conditions. **b** RT–qPCR was performed to detect TMEM237 expression in hypoxic HCC cells with HIF-1α knockdown or HIF-2α knockdown. **c** Western blotting was conducted to measure TMEM237 protein levels in hypoxic HCC cells with HIF-1α knockdown or HIF-2α knockdown. **d** HCC cells treated with a PHD inhibitor (DMOG) were subjected to RT−qPCR and Western blotting for the expression of TMEM237. **e** The luciferase reporter plasmid containing the wild-type (wt) TMEM237 promoter or the corresponding sequence with the HRE mutation (mt) was transfected into HEK293T cells, and the luciferase activity was examined. **f** A ChIP assay was performed to determine the enrichment of HIF-1α in the promoter region of TMEM237. *P < 0.05

Transwell assay

Transwell migration and invasion assays were performed to explore cell migration and invasion ability according to the protocols described in previous studies [23].

In vivo experiments

Four-week-old male BALB/c nude mice were housed under pathogen-free conditions in the Laboratory Animal Center of Xi'an Jiaotong University. Animal experiments were performed according to the protocols approved by the Ethics Review Committee of Xi'an Jiaotong University. The mice were randomly grouped (n = 6 per group) for animal experiments. A subcutaneous xenograft model was established by injecting HCC cells (2×10^6) subcutaneously into the flank of each mouse, and we measured the tumor volume (calculated as $0.5 \times \text{length} \times \text{width} \times \text{width}$) every three days. The mice were sacrificed after three weeks, and the tumor specimens were harvested for further experiments. A pulmonary metastatic model was established by injecting HCC cells (2×10^6) into the tail vein. After six weeks, the lung tissues were collected and subjected to hematoxylin and eosin (H&E) staining, followed by microscopic examination.

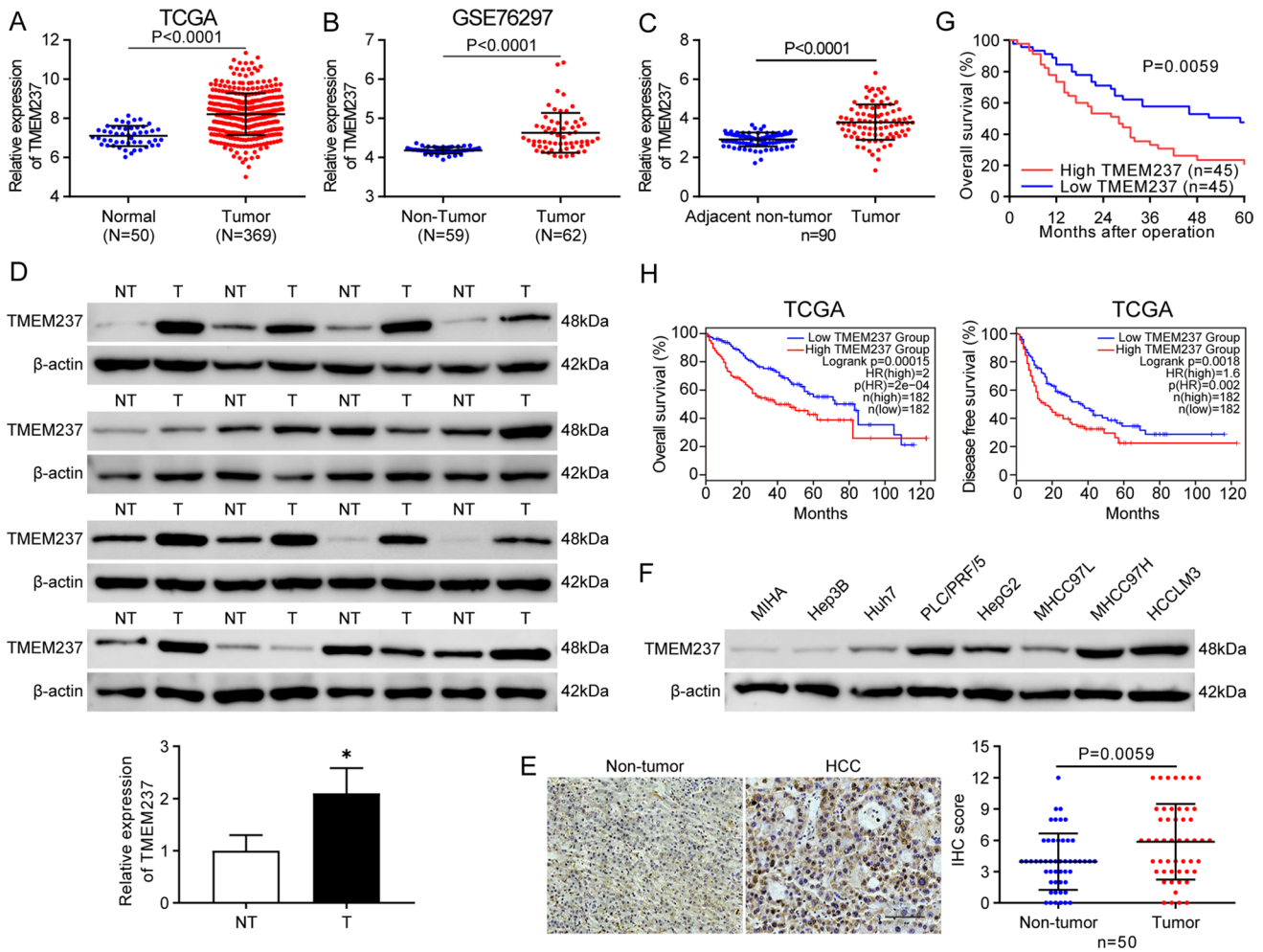

Fig. 2 TMEM237 is highly expressed in HCC. **a** TCGA data were analyzed to determine TMEM237 expression in HCC and normal liver tissues. **b** The expression difference of TMEM237 in HCC and nontumor tissues from the GEO database (GSE76297). **c** RT−qPCR was performed to determine TMEM237 expression in ninety pairs of HCC and the corresponding tumor-adjacent tissues. **d** Sixteen pairs of HCC and corresponding nontumor (NT) tissues were subjected to Western blotting to detect TMEM237 expression. **e** IHC staining was conducted to measure TMEM237 levels in 50 pairs of HCC and nontumor tissues. Scale bar: 100 μm. **f** Western blotting was conducted to determine the levels of TMEM237 in HCC cell lines (Hep3B, Huh7, PLC/PRF/5, HepG2, MHCC97L, MHCC97H, and HCCLM3) and the normal hepatic cell line (MIHA). **g** The overall survival (OS) of HCC patients with high or low TMEM237 levels was analyzed by the Kaplan−Meier method and log-rank test. **h** The OS and disease-free survival (DFS) of HCC patients with high or low TMEM237 levels in the TCGA database. *P < 0.05

Luciferase reporter assays

The wild-type (wt) TMEM237 promoter or the corresponding sequences with mutations (mt) in the predicted HRE were synthesized and cloned into pGL3 vectors. Subsequently, HEK293T cells were transfected with these vectors and cultured under hypoxia for 48 h. The luciferase activities were measured by the Dual-Luciferase Reporter Assay system (Promega Corporation) with Renilla luciferase activity used for normalization.

Chromatin immunoprecipitation (ChIP)

ChIP assays were carried out in accordance with the manufacturer's instructions using the SimpleChIP® Enzymatic Chromatin IP Kit (CST, USA). After incubation under normoxic and hypoxic conditions for 16 h, the cells were cross-linked and sonicated, and then the lysates were incubated with antibodies against HIF-1α or IgG. The immunoprecipitated chromatin was analyzed by RT−qPCR. The primer sequences for the TMEM237 HRE were 5′-GAACCTTTC GCAGATTTCACA (forward) and TTTCCTTGTAGGCCG ATTTG (reverse).

RNA sequencing (RNA-seq)

Total RNA extracted from HCCLM3 cells with or without TMEM237 knockdown was checked for integrity by agarose gel electrophoresis and quantified and qualitatively checked by a NanoDrop ND-100 (Thermo Scientific, USA). Total RNA (1–2 μg) was enriched with the NEBNext® Poly(A) mRNA Magnetic Isolation Module (NEB, USA) for mRNA, and the processed product RNA was used to construct a library with the KAPA Stranded RNA-Seq Library Prep Kit (Illumina, USA). The sequencing libraries of different samples were denatured with 0.1 M NaOH to generate single-stranded DNA and then diluted to a concentration of 8 pM for in situ amplification with the NovaSeq 6000 S4 Reagent Kit (300 cycles, Illumina). The ends of the generated fragments were sequenced with a sequencer (Illumina NovaSeq 6000, 150 paired-end). The raw sequence data reported in this paper have been deposited in the Genome Sequence Archive in National Genomics Data Center, China National Center for Bioinformation/Beijing Institute of Genomics, Chinese Academy of Sciences (GSA-Human: HRA004018) that are publicly accessible at https://ngdc.cncb.ac.cn/gsa-human.

Statistical analysis

Data are presented as the mean ± SD. We used GraphPad Prism software version 8.0 (GraphPad Software, Inc., San Diego, CA, USA) for statistical analysis. Data were compared using a two-tailed Student's t test and ANOVA. The association between TMEM237 expression and clinicopathological features was analyzed using the chi-squared test and Fisher's exact test. The difference in overall survival between the two groups was analyzed using Kaplan−Meier curves and the log-rank test. The variables selected from the univariate analysis were subjected to Cox proportional hazards regression analysis to determine the independent factors that influence overall survival. Pearson correlation analysis was carried out to determine the correlation between HIF-1α, p-Pyk2, p-ERK1/2 and TMEM237 levels. $P < 0.05$ was considered to indicate a statistically significant difference.

Table 2 Univariate and multivariate analysis of factors associated with overall survival in HCC patients

Clinical variables	Univariate analysis		Multivariate analysis	
	HR (95%CI)	P value	HR (95%CI)	P value
Age (≥ 50 vs. < 50 years)	1.233 (0.733–2.074)	0.432		
Gender (female vs. male)	0.828 (0.387–1.771)	0.598		
Tumor size (≥ 5 vs. < 5 cm)	2.195 (1.284–3.753)	0.002*	1.284 (0.547–2.756)	0.541
Tumor number (≥ 2 vs.1)	2.055 (1.114–3.792)	0.006*	1.122 (0.534–2.520)	0.769
TNM stage (III + IV vs. I + II)	3.354 (1.474–7.633)	< 0.001*	2.364 (1.124–5.036)	0.023*
Edmondson–Steiner grading (III + IV vs. I + II)	1.587 (0.854–2.952)	0.096		
Venous infiltration (present vs. absent)	2.115 (1.201–3.726)	0.003*	1.539 (0.853–2.746)	0.147
AFP (≥ 20 vs. < 20 ng/ml)	1.165 (0.652–2.079)	0.615		
HBV infection (present vs. absent)	0.959 (0.529–1.736)	0.887		
TMEM237 expression (high vs. low)	2.037 (1.211–3.427)	0.006*	1.930 (1.117–3.383)	0.019*

HR hazard ratio, *CI* confidence interval

*Statistically significant

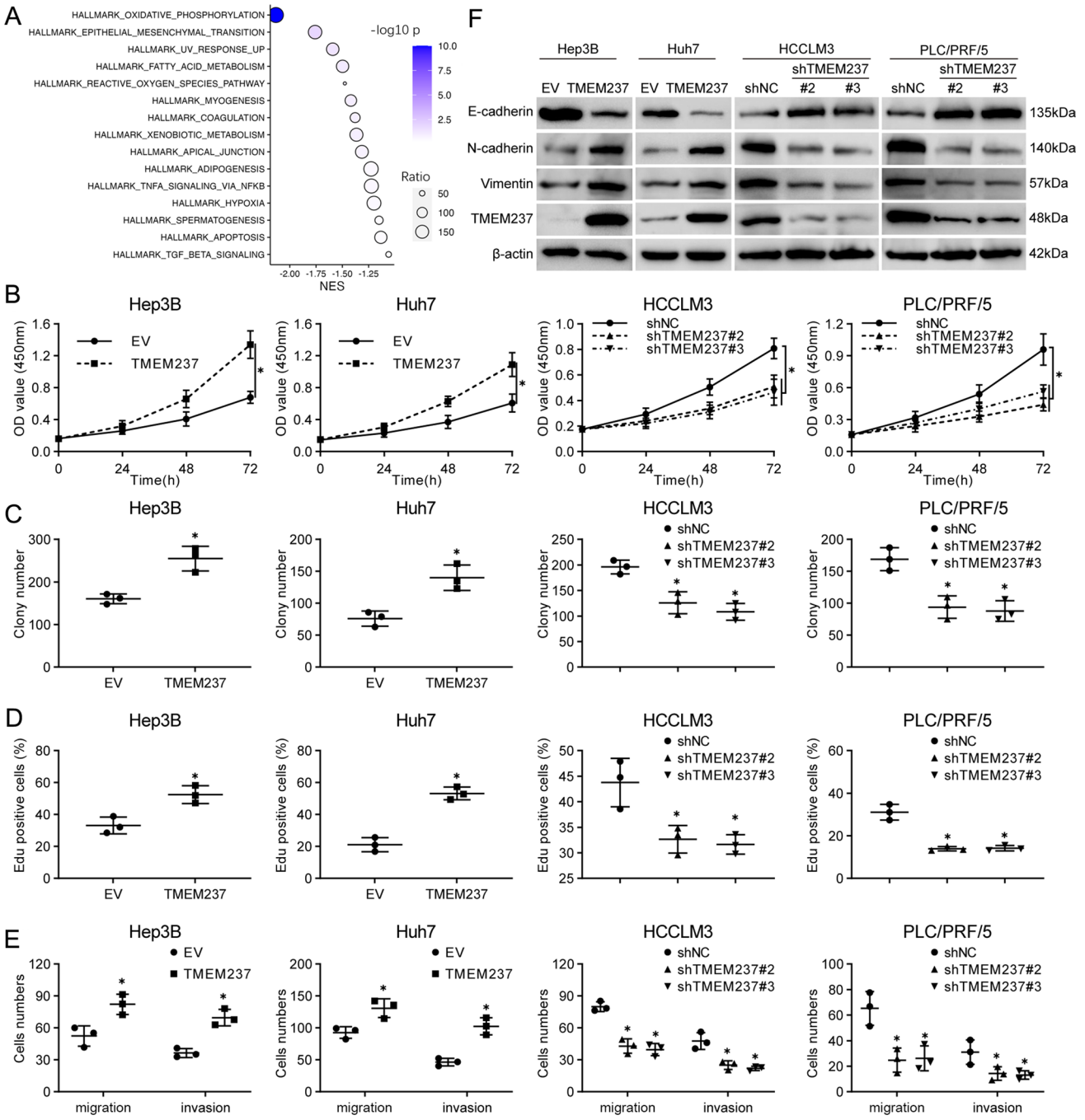

Fig. 3 TMEM237 contributes to HCC cell proliferation, migration and invasion. **a** TMEM237-dependent genes were subjected to gene pathway enrichment analysis. The top 15 categories are shown. **b** CCK-8, **c** colony formation and **d** EdU assays were conducted to evaluate the effects of TMEM237 overexpression and knockdown on the viability and proliferation of HCC cells. **e** Transwell assays were performed to detect the migration and invasion of HCC cells affected by TMEM237 overexpression and knockdown. **f** Western blotting was performed to detect the levels of E-cadherin, N-cadherin and vimentin in HCC cells after TMEM237 overexpression and knockdown. *P < 0.05

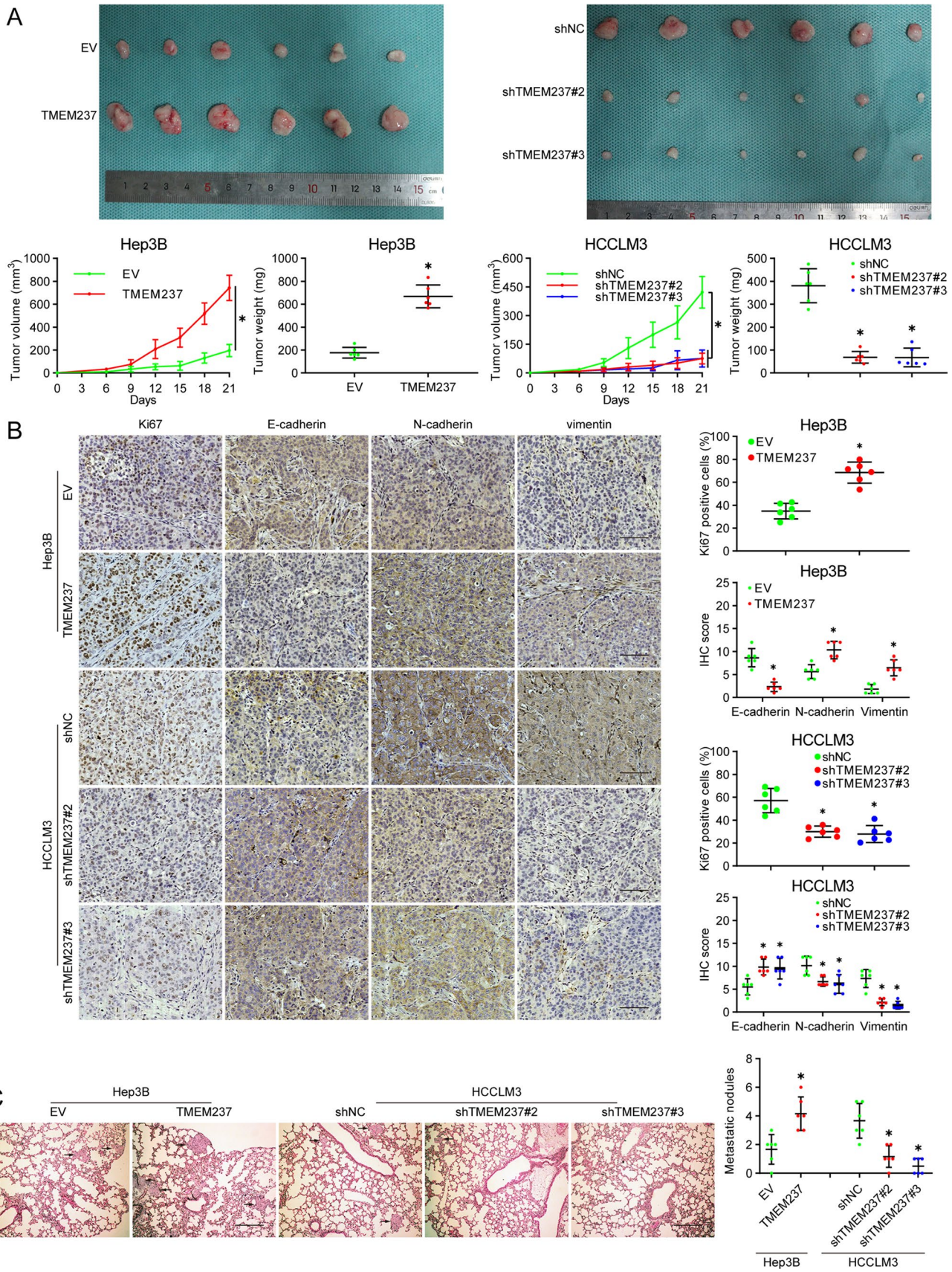
A
EV
TMEM237
shNC
shTMEM237#2
shTMEM237#3
Hep3B
Tumor volume (mm3)
Days
Tumor weight (mg)
HCCLM3
B
Ki67
E-cadherin
N-cadherin
vimentin
Hep3B
HCCLM3
Ki67 positive cells (%)
IHC score
C
Metastatic nodules

◂**Fig. 4** TMEM237 contributes to HCC growth and metastasis in vivo. **a** HCC cells with corresponding vector transfection were subcutaneously injected into the flank of nude mice. The volume of the xenograft tumor was measured every 3 days. The mice were sacrificed 3 weeks after injection, and the tumors were weighed. **b** IHC staining was performed to determine the levels of Ki67, E-cadherin, N-cadherin and vimentin in xenograft tumor tissues. Scale bar: 100 μm. **c** HCC cells with corresponding vector transfection were injected into the tail vein of nude mice. The lung tissues were subjected to H&E staining, and the metastatic nodules were examined microscopically. Scale bar: 300 μm. *P < 0.05

Results

HIF-1α activates TMEM237 transcription in hypoxic HCC cells

We previously investigated hypoxia-induced transcripts in Hep3B cells using a microarray assay [24]. The microarray data (GSE155505) showed that TMEM237 was significantly upregulated in Hep3B cells under hypoxic conditions (Fig. 1a). Then, RT−qPCR and Western blotting assays were conducted to measure TMEM237 levels in Hep3B and HCCLM3 cells cultured under normoxic or hypoxic conditions. The results showed that TMEM237 levels were drastically increased by hypoxia, and knockdown of HIF-1α but not HIF-2α abolished the effects of hypoxia on TMEM237 expression (P < 0.05, Fig. 1b, c). Furthermore, Hep3B and HCCLM3 cells were treated with a PHD inhibitor (DMOG) to mimic hypoxic conditions. The results revealed that DMOG treatment notably upregulated HIF-1α and TMEM237 levels (P < 0.05, Fig. 1d). Additionally, a luciferase reporter assay showed that hypoxia markedly enhanced the transcriptional activity of the TMEM237 promoter, while mutation of the HRE in the TMEM237 promoter abrogated the effects of hypoxia on TMEM237 transcription (P < 0.05, Fig. 1e). Moreover, ChIP assays demonstrated that HIF-1α was recruited to the HRE in the TMEM237 promoter (P < 0.05, Fig. 1f). According to TCGA-LIHC data analysis, although TMEM237 CNV was positively correlated with TMEM237 expression (R = 0.22, P = 2.3e−05, Supplementary Fig. 1A), the correlation between HIF-1α and TMEM237 expression was more significant in HCC tissues (R = 0.58, P = 6.0e−29, Supplementary Fig. 1B). HIF-1α expression was not associated with TMEM237 CNV in HCC tissues (R = 0.094, P = 0.074, Supplementary Fig. 1C). It showed that the majority of tumors (95.65%) in TCGA-LIHC cohort shows no significant copy gain or loss (Supplementary Fig. 1D) and the expression of HIF1A and TMEM237 are positively correlated in both groups with or without TMEM237 copy gains (P < 0.05, Supplementary Fig. 1E and 1F). Therefore, these data suggest that HIF-1α transactivates TMEM237 in hypoxic HCC cells.

TMEM237 is aberrantly overexpressed in HCC

To determine the expression of TMEM237 in HCC, the TCGA and GEO databases were analyzed, and we found that TMEM237 was consistently upregulated in HCC tissues in TCGA datasets (P < 0.0001; Fig. 2a), GSE76297 (P < 0.0001; Fig. 2b) and GSE45436 (P < 0.0001; Supplementary Fig. 2A). Moreover, RT−qPCR was performed on ninety pairs of HCC and corresponding adjacent nontumor tissues, and the results showed that TMEM237 mRNA expression in HCC tissues was significantly elevated compared with that in nontumor tissues (P < 0.0001; Fig. 2c). In addition, Western blotting and IHC assay results revealed that TMEM237 was markedly upregulated in HCC tissues compared to nontumor tissues at the protein level (P < 0.05; Fig. 2d, e). Moreover, TMEM237 was confirmed to be upregulated in HCC cell lines (Huh7, PLC/PRF/5, HepG2, MHCC97L, MHCC97H, and HCCLM3) compared with the immortalized normal hepatocyte cell line MIHA (Fig. 2f). Altogether, these results demonstrate that TMEM237 levels are significantly elevated in HCC.

Elevated TMEM237 expression is correlated with adverse clinical features and a poor prognosis in HCC patients

To determine the correlation between TMEM237 expression and clinical parameters in HCC, our HCC patient cohort was divided into two groups (the high/low TMEM237 groups) based on the median TMEM237 expression in HCC tissues. The data in Table 1 indicated that high TMEM237 expression was associated with large tumor size (P = 0.011), multiple tumors (P = 0.042), advanced TNM stage (P = 0.005) and vascular infiltration (P = 0.003). In addition, analysis of the TCGA database revealed that TMEM237 was more highly expressed in HCC with high tumor grade (G3 + G4) (P < 0.0001; Supplementary Fig. 2B) or advanced tumor stages (III–IV) (P < 0.0001; Supplementary Fig. 2C). Additionally, HCC patients with high TMEM237 levels showed poorer overall survival than those with low TMEM237 levels (P = 0.0059; Fig. 2g). TCGA data from GEPIA2 [25] also verified that high TMEM237 levels were related to worse overall survival (P = 0.00015; Fig. 2h) and disease-free survival (P = 0.0018; Fig. 2h) in HCC patients. However, TMEM237 CNV was not associated with the prognosis of HCC patients (P = 0.59, Supplementary Fig. 2D). Univariate analysis showed that tumor size, tumor number, TNM stage, venous infiltration and TMEM237 expression were notably associated with HCC patient overall survival (P < 0.05; Table 2). Moreover, multivariate analysis showed that TMEM237 expression and TNM stage served as independent prognostic factors for overall survival in HCC (P < 0.05; Table 2).

TMEM237 promotes HCC cell proliferation, migration and invasion in vitro

To explore the biological functions of TMEM237, shNC and shTMEM237 subclones of HCCLM3 cells were subjected to RNA isolation and high-throughput RNA-seq. In response to TMEM237 knockdown, 1011 mRNAs were markedly downregulated, and 1070 mRNAs were significantly upregulated (adjusted $P < 0.01$, $\log_2$ fold change > 2, Supplementary Fig. 3A and 3B). Next, GSEA of TMEM237-induced genes revealed "oxidative phosphorylation" and "epithelial-mesenchymal transition" as the top two categories (Fig. 3a and Supplementary Table 3). Thus, further experiments were performed to investigate the regulatory role of TMEM237 in HCC growth and metastasis. We established stable TMEM237 overexpression in Hep3B and Huh7 cell lines with relatively low endogenous TMEM237 levels and knockdown in HCCLM3 and PLC/PRF/5 cell lines with relatively high endogenous TMEM237 levels (Supplementary Fig. 4). CCK-8, colony formation and EdU assays showed that TMEM237 overexpression drastically increased Hep3B and Huh7 cell viability and promoted cell proliferation, while TMEM237 knockdown strikingly decreased the viability and suppressed the proliferation of HCCLM3 and PLC/PRF/5 cells ($P < 0.05$; Fig. 3b–d and Supplementary Fig. 5A and 5B). Transwell assays revealed that the migration and invasion ability of Hep3B and Huh7 cells was markedly enhanced by TMEM237 overexpression, whereas the migration and invasion potential of HCCLM3 and PLC/PRF/5 cells was significantly decreased with TMEM237 knockdown ($P < 0.05$; Fig. 3e and Supplementary Fig. 5C). Western blotting assays were performed to detect the effects of TMEM237 on the EMT process in HCC cells. The results showed that TMEM237 overexpression markedly decreased the expression of an epithelial marker (E-cadherin) and upregulated the mesenchymal markers N-cadherin and vimentin in Hep3B and Huh7 cells, while TMEM237 knockdown markedly suppressed EMT in HCCLM3 and PLC/PRF/5 cells (Fig. 3f). Thus, these data verify that TMEM237 promotes HCC cell proliferation, migration, invasion and EMT.

TMEM237 contributes to HCC growth and metastasis in vivo

To determine the effects of TMEM237 on HCC growth in vivo, Hep3B cells with TMEM237 overexpression or HCCLM3 cells with TMEM237 knockdown and corresponding control cells were subcutaneously injected into nude mice. The volume and weight of tumors formed by Hep3B cells overexpressing TMEM237 were significantly increased compared with those of tumors formed by control Hep3B cells ($P < 0.05$; Fig. 4a). In contrast, TMEM237 knockdown in HCCLM3 cells led to robust tumor growth restriction in mice ($P < 0.05$; Fig. 4a). Then, the xenograft tumor tissues were examined by IHC staining. The results showed that xenograft tumors derived from Hep3B cells overexpressing TMEM237 exhibited dramatically higher Ki67, N-cadherin and vimentin staining and lower E-cadherin staining than those derived from control cells ($P < 0.05$; Fig. 4b). However, Ki67, N-cadherin and vimentin levels were lower and E-cadherin levels were higher in xenograft tumors from HCCLM3 cells with TMEM237 knockdown compared with the control group ($P < 0.05$; Fig. 4b). Then, a pulmonary metastatic model was established to determine the effects of TMEM237 on HCC metastasis in vivo. We discovered that TMEM237 overexpression markedly increased the number of metastatic nodules in the lung tissues of mice ($P < 0.05$; Fig. 4c). Moreover, fewer foci were found in the lungs of mice in the TMEM237 knockdown group than in the lungs of mice the control group ($P < 0.05$; Fig. 4c). Therefore, these data indicate that TMEM237 contributes to HCC growth and metastasis in vivo.

TMEM237 interacts with NPHP1 to activate the Pyk2/ERK1/2 pathway

To unravel the underlying mechanisms by which TMEM237 exerts an oncogenic role in HCC, HCCLM3 cell lysates were immunoprecipitated by a TMEM237 antibody, followed by mass spectrometric analysis (Fig. 5a). The results identified NPHP1 as a potential protein interacting with TMEM237 (Fig. 5a and Supplementary Fig. 6). Thus, co-IP assays were performed to determine the interaction between TMEM237 and NPHP1. Antibodies against TMEM237 but not IgG immunoprecipitated NPHP1 from HCCLM3 lysates (Fig. 5b). Reciprocally, the anti-NPHP1 antibody immunoprecipitated TMEM237 from HCCLM3 lysates (Fig. 5b). Furthermore, FLAG-tagged TMEM237 and HA-tagged NPHP1 were coexpressed in HEK293T cells, and co-IP assays were conducted with anti-FLAG and anti-HA antibodies. The results validated the interaction between exogeneous TMEM237 and NPHP1 (Fig. 5c). Thus, we speculated that NPHP1 might be involved in the molecular mechanism underlying the biological function of TMEM237 in HCC. A previous study reported that NPHP1 interacts with Pyk2 and triggers the phosphorylation of Pyk2, subsequently activating the Pyk2/ERK1/2 pathway in tubular epithelial cells [26]. Our RNA-seq data revealed that the gene expression of proteins interacting with MAPK1 was markedly changed by TMEM237 knockdown ($P < 0.05$, Fig. 5d and Supplementary Fig. 7), indicating the regulatory role of TMEM237 in the ERK pathway. We performed Co-IP with an antibody against TMEM237, and both NPHP1 and Pyk2 were detected in

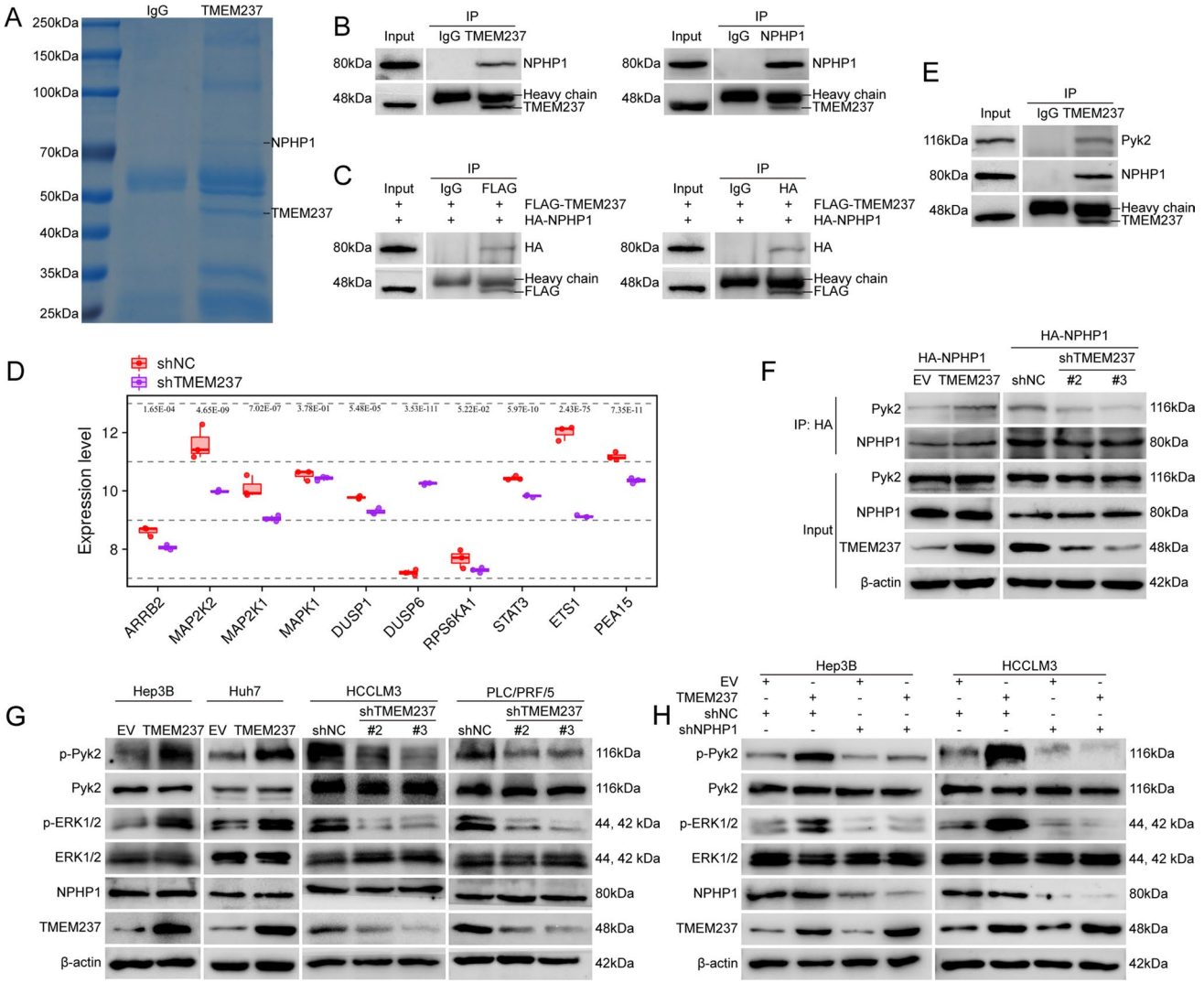

Fig. 5 TMEM237 interacts with NPHP1 to activate the Pyk2/ERK1/2 pathway. **a** HCCLM3 cell lysates were immunoprecipitated with a TMEM237 antibody, followed by mass spectrometric analysis. **b** Co-IP assays were performed to detect the interaction between TMEM237 and NPHP1 in HCCLM3 cells. **c** Co-IP assays were performed to detect the interaction between exogenous TMEM237 and NPHP1 in HEK293T cells. **d** NPHP1 and Pyk2 were immunoprecipitated by antibodies against TMEM237 in cell lysates. **e** The gene expression of proteins interacting with MAPK1 was markedly changed by TMEM237 knockdown, as indicated by RNA-seq data. **f** Co-IP assays were conducted to determine the effects of TMEM237 on the interaction between NPHP1 and Pyk2 in HCC cells. **g** Western blotting was performed to determine the effects of TMEM237 on Pyk2/ERK1/2 pathway activation in HCC cells. **h** Western blotting was performed to evaluate the role of NPHP1 in TMEM237-induced Pyk2/ERK1/2 pathway activation

the immunoprecipitates from HCCLM3 lysates (Fig. 5e), indicating that TMEM237 forms a protein complex with NPHP1 and Pyk2. Furthermore, co-IP assays were conducted to determine the effects of TMEM237 on the interaction of NPHP1 and Pyk2. The results suggested that TMEM237 overexpression enhanced, while TMEM237 knockdown repressed, the interaction between NPHP1 and Pyk2 (Fig. 5f). Given that NPHP1 is required for Pyk2 phosphorylation, we determined the effects of TMEM237 on p-Pyk2 and p-ERK1/2 levels. The results revealed that the overexpression of TMEM237 increased the phosphorylation levels of Pyk2 and ERK1/2, whereas TMEM237 knockdown notably reduced the activities of Pyk2 and ERK1/2 in HCC cells (Fig. 5g). Additionally, the knockdown of NPHP1 markedly counteracted the promotive effects of TMEM237 overexpression on the p-Pyk2 and p-ERK1/2 levels in Hep3B and HCCLM3 cells (Fig. 5h). Thus, these data prove that TMEM237 forms a complex with NPHP1 and Pyk2 to reinforce Pyk2 phosphorylation mediated by NPHP1, thereby activating the Pyk2/ERK1/2 pathway in HCC cells.

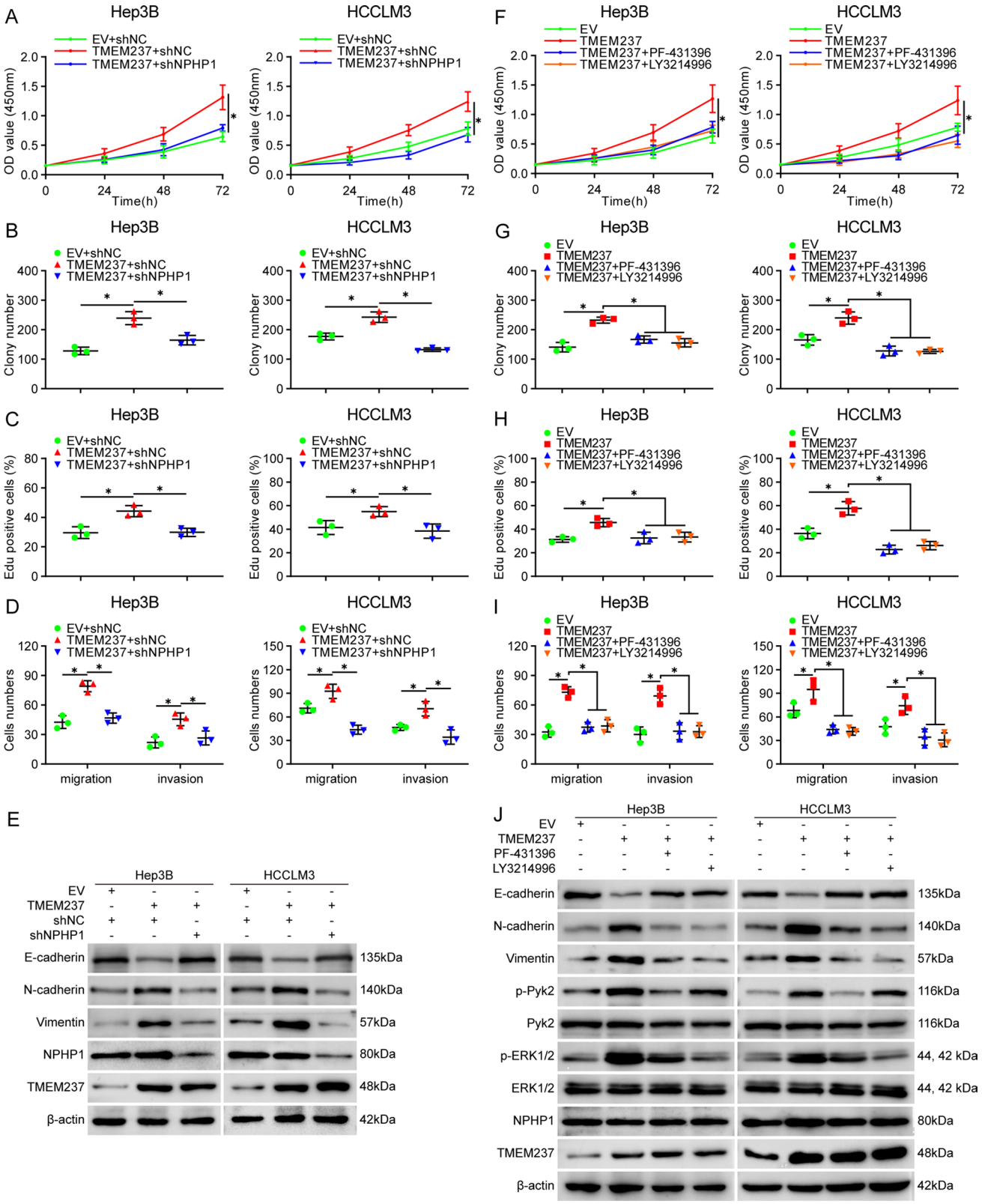
A
Hep3B
HCCLM3
EV+shNC
TMEM237+shNC
TMEM237+shNPHP1
OD value (450nm)
Time(h)
F
EV
TMEM237
TMEM237+PF-431396
TMEM237+LY3214996
B
Clony number
G
C
Edu positive cells (%)
H
D
Cells numbers
migration
invasion
I
E
shNC
shNPHP1
E-cadherin
N-cadherin
Vimentin
NPHP1
TMEM237
β-actin
135kDa
140kDa
57kDa
80kDa
48kDa
42kDa
J
PF-431396
LY3214996
p-Pyk2
Pyk2
p-ERK1/2
ERK1/2
116kDa
44, 42 kDa

◂**Fig. 6** The NPHP1/Pyk2/ERK1/2 pathway mediates the biological function of TMEM237 in HCC cells. Hep3B and HCCLM3 cells overexpressing TMEM237 were transfected with NPHP1 shRNA (shNPHP1) or nontargeting shRNA (shNC). **a** CCK-8, **b** colony formation, **c** EdU, **d** transwell and **e** Western blotting assays were employed to examine the proliferation, migration, invasion and EMT process of HCC cells in the indicated groups. Hep3B and HCCLM3 cells overexpressing TMEM237 were treated with a Pyk2 inhibitor (PF-431396) or an ERK1/2 inhibitor (LY3214996). **f** CCK-8, **g** colony formation, **h** EdU, **i** transwell and **j** Western blotting assays were employed to assess the proliferation, migration, invasion and EMT of HCC cells in the indicated groups. Scale bar: 50 μm for the EdU results and 200 μm for the transwell results. *$P < 0.05$

The NPHP1/Pyk2/ERK1/2 pathway mediates the role of TMEM237 in HCC cells

Next, we determined whether NPHP1 mediated the biological function of TMEM237 in Hep3B and HCCLM3 cells. CCK-8, colony formation and EdU assays revealed that NPHP1 knockdown offset the effects of TMEM237 on HCC cell proliferation ($P < 0.05$; Fig. 6a–c and Supplementary Fig. 8A and 8B). Additionally, transwell assays suggested that the increases in migration and invasion of HCC cells induced by TMEM237 were attenuated by NPHP1 knockdown ($P < 0.05$; Fig. 6d and Supplementary Fig. 8C). Moreover, NPHP1 knockdown reversed the EMT process induced by TMEM237 overexpression in HCC cells (Fig. 6e). Altogether, these results indicate that NPHP1 mediates the biological function of TMEM237 in HCC cells.

Furthermore, Hep3B and HCCLM3 cells were treated with a Pyk2 inhibitor (PF-431396) and ERK1/2 inhibitor (LY3214996) to examine whether the Pyk2/ERK1/2 pathway is involved in the role of TMEM237 in HCC. CCK-8, colony formation and EdU assays suggested that both PF-431396 and LY3214996 blocked the effects of TMEM237 on HCC cell proliferation ($P < 0.05$; Fig. 6f–h and Supplementary Fig. 8D and 8E). In addition, transwell and Western blotting assays showed that the TMEM237-induced migration, invasion and EMT of Hep3B and HCCLM3 cells were abrogated by PF-431396 and LY3214996 ($P < 0.05$; Fig. 6i, j and Supplementary Fig. 8F). Collectively, we demonstrate that the NPHP1/Pyk2/ERK1/2 pathway mediates the oncogenic effect of TMEM237 in HCC.

Hypoxia-induced TMEM237 activates the Pyk2/ERK1/2 pathway in HCC

Previous studies indicate that hypoxia activates the Pyk2/ERK1/2 pathway [27, 28]. Hence, we hypothesized that TMEM237 might be involved in the hypoxia-activated Pyk2/ERK1/2 pathway. To validate this hypothesis, Hep3B and HCCLM3 cells with TMEM237 knockdown were cultured under hypoxic conditions, and the Western blotting results revealed that TMEM237 knockdown attenuated the hypoxia-induced phosphorylation of Pyk2 and ERK1/2 (Fig. 7a). In addition, knockdown of NPHP1 blocked the effects of hypoxia on the activation of the Pyk2/ERK1/2 pathway in Hep3B and HCCLM3 cells (Fig. 7b). Furthermore, the HCC tissues were divided into a high TMEM237 group (IHC score > 3, n = 35) and a low TMEM237 group (IHC score ≤ 3, n = 15). Then, we detected the levels of HIF-1α, NPHP1, p-Pyk2 and p-ERK1/2 in HCC tissues with IHC staining, and the results showed that HIF-1α, p-Pyk2 and p-ERK1/2 levels were much higher in the high TMEM237 group ($P < 0.05$; Fig. 7c). Moreover, the levels of HIF-1α, p-Pyk2 and p-ERK1/2 were positively correlated with TMEM237 expression ($P < 0.05$; Supplementary Fig. 9). Additionally, IHC staining results revealed that TMEM237 overexpression increased p-Pyk2 and p-ERK1/2 levels, while TMEM237 knockdown decreased the levels of p-Pyk2 and p-ERK1/2 in xenograft tumor tissues ($P < 0.05$; Fig. 7d). In summary, we demonstrate that hypoxia-induced TMEM237 expression activates the Pyk2/ERK1/2 signaling pathway in an NPHP1-dependent manner in HCC.

Discussion

A hypoxic microenvironment is a ubiquitous feature of solid tumors due to extremely fast tumor growth and insufficient neovascularization; the hypoxic status of the microenvironment leads a series of pathophysiological changes in tumor cells, accelerating the malignant progression of tumors, and resulting in a poor prognosis of patients [29]. The biological responses of hypoxic tumor cells are primarily mediated by HIFs, which include O_2-regulated HIF-α and constitutively expressed HIF-1β. HIF-α family members are the key regulators of HIF activity and predominantly include HIF-1α and HIF-2α. HIF-α proteins are hydroxylated by PDH with O_2 as a substrate and subsequently degraded; therefore, the hydroxylation modification of HIF-α is inhibited, and HIF-α accumulates in the hypoxic microenvironment [5]. As a transcription factor, HIF-α dimerizes with HIF-1β and is recruited to the HRE in the promoter region to activate the transcription of target genes. Cofilin1, which is transcriptionally activated by HIF-1α, activates AKT signaling by inhibiting the degradation of PLD1, which ultimately contributes to HCC growth and metastasis [7]. The HIF signaling pathway is one of the most promising targets for precision therapy of HCC [30]. ADRB2 maintains HIF-1α protein stability by negatively regulating autophagy, thereby facilitating HCC growth and sorafenib resistance [31]. tRNA methyltransferase 5 (TRMT5) inhibits the proliferation and metastasis of HCC cells by reducing HIF-1α protein stability [32]. Ursodeoxycholic acid (UDCA) suppresses the expression and transcriptional activity of HIF-1α and subsequently reduces VEGF and IL-8 levels, which attenuates hypoxic

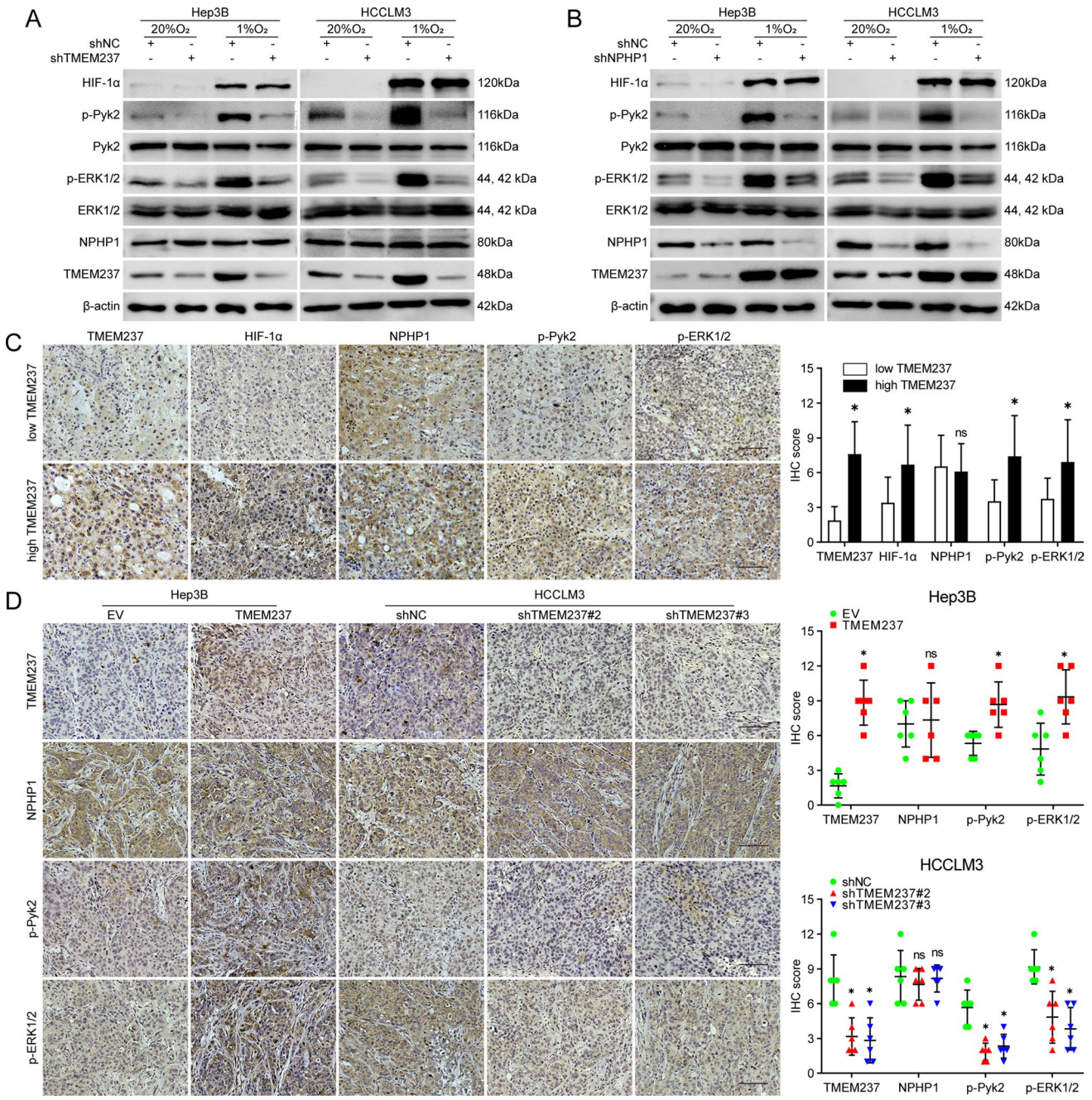

Fig. 7 TMEM237 is involved in hypoxia-induced Pyk2/ERK1/2 pathway activation. **a** The effects of TMEM237 knockdown on hypoxia-induced Pyk2/ERK1/2 pathway activation in HCC cells were determined by Western blotting. **b** The impact of NPHP1 knockdown on hypoxia-induced Pyk2/ERK1/2 pathway activation in HCC cells was evaluated by Western blotting. **c** IHC staining was conducted to detect the levels of HIF-1α, NPHP1, p-Pyk2 and p-ERK1/2 in HCC tissues with high or low TMEM237 expression. **d** IHC staining was performed to examine TMEM237, NPHP1, p-Pyk2 and p-ERK1/2 levels in xenograft tumor tissues. *P < 0.05

HCC cell-induced angiogenesis [33]. Asparagus polysaccharide (ASP) represses HIF-1α and VEGF expression by inactivating the MAPK and PI3K signaling pathways, thereby attenuating hypoxia-driven HCC progression [34]. Therefore, an in-depth study of the molecular regulatory mechanism involving HIF will help to develop new strategies for the diagnosis and treatment of HCC.

Although many proteins induced by hypoxia have been reported to be involved in tumor progression [35, 36], many proteins that might be regulated by HIF remain

largely elusive. In the present study, we identified that TMEM237 was dramatically upregulated in hypoxic Hep3B cells by analyzing our previous microarray data. Then, RT−qPCR and Western blotting results verified that TMEM237 was increased by hypoxia in HCC cells and that this effect was mediated by HIF-1α but not HIF-2α. Next, we found that the PHD inhibitor DMOG also led to elevated TMEM237 mRNA and protein levels. Then, we demonstrated that HIF-1α recognized the HRE in the promoter region of TMEM237 and positively regulated its transcription. Thus, we identified TMEM237 as a novel hypoxia-responsive gene that is transcriptionally activated by HIF-1α.

Next, we analyzed TMEM237 expression by RT−qPCR, Western blotting and IHC staining and found that TMEM237 expression in HCC tissues was significantly higher than that in the corresponding nontumor tissues. TMEM237 overexpression in HCC tissues was closely associated with adverse clinical features, such as large tumor size, multiple tumors, vascular invasion and advanced TNM stage. Importantly, HCC patients with high TMEM237 expression in tumor tissues had a worse prognosis than those with low TMEM237 expression. Multivariate analysis identified TMEM237 expression as an independent prognostic factor for HCC patients. In summary, these data inspired us to hypothesize that TMEM237 might exert an oncogenic role in HCC. RNA-seq data analysis suggested that TMEM237-induced genes were implicated in oxidative phosphorylation and EMT. Thus, loss- and gain-of-function experiments showed that TMEM237 promoted HCC cell proliferation, motility and EMT. We further verified that TMEM237 contributes to the growth and lung metastasis of HCC in vivo. Previous studies have mainly investigated the association of TMEM237 with Joubert syndrome [22, 37]. A recent study demonstrates that TMEM237 enhances the stability of human riboflavin transporter-3 (hRFVT-3) in human intestinal epithelial HuTu-80 cells [38]. Thus, we identified TMEM237 as an oncogene in HCC for the first time.

Then, proteins from HCCLM3 cells were immunoprecipitated with an anti-TMEM237 antibody, and NPHP1 was identified by mass spectrometry as a potential protein interacting with TMEM237. Previous studies reported that NPHP1 mutation is associated with nephronophthisis [39], and TMEM237 is closely related to Joubert syndrome-related disorders (JSRDs) [22]. Nephronophthisis and JSRDs are ciliopathies and phenotypically overlap with each other [22], which implies a functional correlation between TMEM237 and NPHP1. Co-IP verified the interaction between endogenous or exogenous TMEM237 and NPHP1 protein. Given that NPHP1 interacts with Pyk2 and activates the Pyk2/ERK1/2 pathway in tubular epithelial cells [26], we detected the interaction between TMEM237 and Pyk2 in HCC cells and found that TMEM237 formed a complex with NPHP1 and Pyk2. In addition, TMEM237 potentiated the interaction between NPHP1 and Pyk2 in HCC cells. Then, we demonstrated that TMEM237 induced the activation of the Pyk2/ERK1/2 pathway in an NPHP1-dependent manner and that the Pyk2/ERK1/2 pathway mediated the effects of TMEM237 on the proliferation, motility and EMT of HCC cells. Therefore, we concluded that TMEM237 modulates the activation of the Pyk2/ERK1/2 pathway by interacting with NPHP1 and that the NPHP1/Pyk2/ERK1/2 pathway mediates the biological function of TMEM237 in HCC cells.

Recent studies have shown that hypoxia induces Pyk2/ERK1/2 pathway activation in human diseases, including cancer [27, 28, 40, 41]. Based on the obtained results, we hypothesized that TMEM237 might be involved in the effects of hypoxia on the activation of the Pyk2/ERK1/2 pathway. The results showed that TMEM237 knockdown significantly offset hypoxia-induced Pyk2/ERK1/2 pathway activation. Intriguingly, neither hypoxia nor TMEM237 knockdown altered NPHP1 levels, which indicated that TMEM237 induced Pyk2/ERK1/2 pathway activation by modulating the interaction of NPHP1 and Pyk2 but not by regulating NPHP1 expression. Additionally, NPHP1 knockdown counteracted the hypoxia-induced phosphorylation of Pyk2 and ERK1/2, further substantiating the indispensable role of NPHP1 in the effects of hypoxia on the Pyk2/ERK1/2 pathway. Moreover, TMEM237 expression was positively correlated with the levels of HIF-1α, p-Pyk2 and p-ERK1/2 in HCC tissues, and TMEM237 increased p-Pyk2 and p-ERK1/2 expression in xenograft tumor tissues. Therefore, we corroborated that the TMEM237/NPHP1 axis mediates hypoxia-induced activation of the Pyk2/ERK1/2 pathway.

In conclusion, we identified a novel HIF-1α-activated gene, TMEM237, that is aberrantly upregulated in HCC and correlated with an unfavorable prognosis in HCC patients. Additionally, we found that TMEM237 interacts with NPHP1 and strengthens the interaction between NPHP1 and Pyk2, thereby triggering the phosphorylation of Pyk2 and ERK1/2. The NPHP1/Pyk2/ERK1/2 pathway mediates the promoting effect of TMEM237 on HCC growth and metastasis.

Supplementary Information The online version contains supplementary material available at https://doi.org/10.1007/s00018-023-04767-y.

Author contributions KT and QL conceived and designed the experiments; TC, LW, CC, RL, NZ, RL, and YN performed the experiments; TC, HL and ZX analyzed the data; HL and ZX contributed reagents/materials/analysis tools; TC and KT wrote the paper. All authors read and approved the final manuscript.

Funding This study was supported by grants from the National Natural Science Foundation of China (82203759), Nature Science Basic Research Program of Shaanxi (2020JC-36), Key Research and Development Program of Shaanxi (2023-YBSF-149), Innovation Capacity Support Plan in Shaanxi Province of China (2023KJXX-107) and Fundamental Research Funds for the Central Universities (xzy012022095).

Availability of data and materials All data generated or analyzed during this study are included either in this article or in the supplementary information files.

Declarations

Conflict of interest The authors declare that they have no competing interests.

Ethics approval and consent to participate All procedures performed in studies involving human participants were in accordance with the ethical standards of the Research Ethics Committee of The First Affiliated Hospital of Xi'an Jiaotong University and with the 1964 Helsinki declaration and its later amendments. All written informed consent to participate in the study was obtained from HCC patients for samples to be collected from them.

Consent for publication Not applicable.

References

1. Sung H, Ferlay J, Siegel RL, Laversanne M, Soerjomataram I, Jemal A, Bray F (2021) Global cancer statistics 2020: GLOBOCAN estimates of incidence and mortality worldwide for 36 cancers in 185 countries. CA Cancer J Clin 71:209–249
2. Llovet JM, Kelley RK, Villanueva A, Singal AG, Pikarsky E, Roayaie S, Lencioni R, Koike K, Zucman-Rossi J, Finn RS (2021) Hepatocellular carcinoma. Nat Rev Dis Primers 7:6
3. Chan AWH, Zhong J, Berhane S, Toyoda H, Cucchetti A, Shi K, Tada T, Chong CCN, Xiang BD, Li LQ et al (2018) Development of pre and post-operative models to predict early recurrence of hepatocellular carcinoma after surgical resection. J Hepatol 69:1284–1293
4. Gilkes DM, Semenza GL, Wirtz D (2014) Hypoxia and the extracellular matrix: drivers of tumour metastasis. Nat Rev Cancer 14:430–439
5. Prabhakar NR, Semenza GL (2015) Oxygen sensing and homeostasis. Physiology (Bethesda) 30:340–348
6. Xiong XX, Qiu XY, Hu DX, Chen XQ (2017) Advances in hypoxia-mediated mechanisms in hepatocellular carcinoma. Mol Pharmacol 92:246–255
7. Yao B, Li Y, Chen T, Niu Y, Wang Y, Yang Y, Wei X, Liu Q, Tu K (2021) Hypoxia-induced cofilin 1 promotes hepatocellular carcinoma progression by regulating the PLD1/AKT pathway. Clin Transl Med 11:e366
8. Wang Y, Lyu Y, Tu K, Xu Q, Yang Y, Salman S, Le N, Lu H, Chen C, Zhu Y et al (2021) Histone citrullination by PADI4 is required for HIF-dependent transcriptional responses to hypoxia and tumor vascularization. Sci Adv 7:eabe3771
9. Sun L, Wang L, Chen T, Shi Y, Yao B, Liu Z, Wang Y, Li Q, Liu R, Niu Y et al (2020) LncRNA RUNX1-IT1 which is downregulated by hypoxia-driven histone deacetylase 3 represses proliferation and cancer stem-like properties in hepatocellular carcinoma cells. Cell Death Dis 11:95
10. Chen T, Liu R, Niu Y, Mo H, Wang H, Lu Y, Wang L, Sun L, Wang Y, Tu K, Liu Q (2021) HIF-1alpha-activated long non-coding RNA KDM4A-AS1 promotes hepatocellular carcinoma progression via the miR-411-5p/KPNA2/AKT pathway. Cell Death Dis 12:1152
11. Wang L, Sun L, Liu R, Mo H, Niu Y, Chen T, Wang Y, Han S, Tu K, Liu Q (2021) Long non-coding RNA MAPKAPK5-AS1/PLAGL2/HIF-1alpha signaling loop promotes hepatocellular carcinoma progression. J Exp Clin Cancer Res 40:72
12. Babcock JJ, Li M (2014) Deorphanizing the human transmembrane genome: a landscape of uncharacterized membrane proteins. Acta Pharmacol Sin 35:11–23
13. Marx S, Dal Maso T, Chen JW, Bury M, Wouters J, Michiels C, Le Calve B (2020) Transmembrane (TMEM) protein family members: poorly characterized even if essential for the metastatic process. Semin Cancer Biol 60:96–106
14. Schmit K, Michiels C (2018) TMEM proteins in cancer: a review. Front Pharmacol 9:1345
15. Shiraishi T, Ikeda K, Tsukada Y, Nishizawa Y, Sasaki T, Ito M, Kojima M, Ishii G, Tsumura R, Saijou S et al (2021) High expression of TMEM180, a novel tumour marker, is associated with poor survival in stage III colorectal cancer. BMC Cancer 21:302
16. Cheng Z, Guo J, Chen L, Luo N, Yang W, Qu X (2015) Overexpression of TMEM158 contributes to ovarian carcinogenesis. J Exp Clin Cancer Res 34:75
17. Zhang S, Dai H, Li W, Wang R, Wu H, Shen M, Hu Y, Xie L, Xing Y (2021) TMEM116 is required for lung cancer cell motility and metastasis through PDK1 signaling pathway. Cell Death Dis 12:1086
18. Zhang TM, Liao L, Yang SY, Huang MY, Zhang YL, Deng L, Hu SY, Yang F, Zhang FL, Shao ZM, Li DQ (2023) TOLLIP-mediated autophagic degradation pathway links the VCP-TMEM63A-DERL1 signaling axis to triple-negative breast cancer progression. Autophagy 19:805–821
19. Duan J, Qian Y, Fu X, Chen M, Liu K, Liu H, Yang J, Liu C, Chang Y (2021) TMEM106C contributes to the malignant characteristics and poor prognosis of hepatocellular carcinoma. Aging (Albany NY) 13:5585–5606
20. Rao J, Wu X, Zhou X, Deng R, Ma Y (2020) TMEM205 is an independent prognostic factor and is associated with immune cell infiltrates in hepatocellular carcinoma. Front Genet 11:575776
21. Zuniga FI, Craft CM (2010) Deciphering the structure and function of Als2cr4 in the mouse retina. Investig Ophthalmol Vis Sci 51:4407–4415
22. Huang L, Szymanska K, Jensen VL, Janecke AR, Innes AM, Davis EE, Frosk P, Li C, Willer JR, Chodirker BN et al (2011) TMEM237 is mutated in individuals with a Joubert syndrome related disorder and expands the role of the TMEM family at the ciliary transition zone. Am J Hum Genet 89:713–730
23. Chen T, Sun L, Yao B, Wang L, Wang Y, Niu Y, Liu R, Mo H, Liu Z, Tu K, Liu Q (2020) MicroRNA-875-5p inhibits tumor growth and metastasis of hepatocellular carcinoma by targeting eukaryotic translation initiation factor 3 subunit a. Oncol Rep 44:2067–2079
24. Gao S, Chen T, Li L, Liu X, Liu Y, Zhao J, Lu Q, Zeng Z, Xu Q, Huang D, Tu K (2020) Hypoxia-inducible ubiquitin specific peptidase 13 contributes to tumor growth and metastasis via enhancing the toll-like receptor 4/myeloid differentiation primary response gene 88/nuclear factor-kappaB pathway in hepatocellular carcinoma. Front Cell Dev Biol 8:587389
25. Tang Z, Kang B, Li C, Chen T, Zhang Z (2019) GEPIA2: an enhanced web server for large-scale expression profiling and interactive analysis. Nucleic Acids Res 47:W556–W560
26. Benzing T, Gerke P, Hopker K, Hildebrandt F, Kim E, Walz G (2001) Nephrocystin interacts with Pyk2, p130(Cas), and tensin and triggers phosphorylation of Pyk2. Proc Natl Acad Sci USA 98:9784–9789
27. Revuelta-Lopez E, Castellano J, Roura S, Galvez-Monton C, Nasarre L, Benitez S, Bayes-Genis A, Badimon L, Llorente-Cortes V (2013) Hypoxia induces metalloproteinase-9 activation and human vascular smooth muscle cell migration through low-density lipoprotein receptor-related protein 1-mediated Pyk2 phosphorylation. Arterioscler Thromb Vasc Biol 33:2877–2887

28. Chen J, Wang Y, Zhang W, Zhao D, Zhang L, Fan J, Li J, Zhan Q (2020) Membranous NOX5-derived ROS oxidizes and activates local Src to promote malignancy of tumor cells. Signal Transduct Target Ther 5:139
29. Schito L, Semenza GL (2016) Hypoxia-inducible factors: master regulators of cancer progression. Trends Cancer 2:758–770
30. Mendez-Blanco C, Fondevila F, Garcia-Palomo A, Gonzalez-Gallego J, Mauriz JL (2018) Sorafenib resistance in hepatocarcinoma: role of hypoxia-inducible factors. Exp Mol Med 50:134
31. Wu FQ, Fang T, Yu LX, Lv GS, Lv HW, Liang D, Li T, Wang CZ, Tan YX, Ding J et al (2016) ADRB2 signaling promotes HCC progression and sorafenib resistance by inhibiting autophagic degradation of HIF1alpha. J Hepatol 65:314–324
32. Zhao Q, Zhang L, He Q, Chang H, Wang Z, Cao H, Zhou Y, Pan R, Chen Y (2023) Targeting TRMT5 suppresses hepatocellular carcinoma progression via inhibiting the HIF-1alpha pathways. J Zhejiang Univ Sci B 24:50–63
33. Lin W, Li S, Meng Y, Huang G, Liang S, Du J, Liu Q, Cheng B (2021) UDCA inhibits hypoxic hepatocellular carcinoma cell-induced angiogenesis through suppressing HIF-1alpha/VEGF/IL-8 intercellular signaling. Front Pharmacol 12:755394
34. Cheng W, Cheng Z, Weng L, Xing D, Zhang M (2021) Asparagus polysaccharide inhibits the hypoxia-induced migration, invasion and angiogenesis of hepatocellular carcinoma cells partly through regulating HIF1alpha/VEGF expression via MAPK and PI3K signaling pathway. J Cancer 12:3920–3929
35. Zheng Y, Huang C, Lu L, Yu K, Zhao J, Chen M, Liu L, Sun Q, Lin Z, Zheng J et al (2021) STOML2 potentiates metastasis of hepatocellular carcinoma by promoting PINK1-mediated mitophagy and regulates sensitivity to lenvatinib. J Hematol Oncol 14:16
36. Fernandez-Palanca P, Payo-Serafin T, San-Miguel B, Mendez-Blanco C, Tunon MJ, Gonzalez-Gallego J, Mauriz JL (2022) Hepatocellular carcinoma cells loss lenvatinib efficacy in vitro through autophagy and hypoxia response-derived neuropilin-1 degradation. Acta Pharmacol Sin https://doi.org/10.1038/s41401-022-01021-2
37. Lambacher NJ, Bruel AL, van Dam TJ, Szymanska K, Slaats GG, Kuhns S, McManus GJ, Kennedy JE, Gaff K, Wu KM et al (2016) TMEM107 recruits ciliopathy proteins to subdomains of the ciliary transition zone and causes Joubert syndrome. Nat Cell Biol 18:122–131
38. Sabui S, Subramanian VS, Pham Q, Said HM (2019) Identification of transmembrane protein 237 as a novel interactor with the intestinal riboflavin transporter-3 (RFVT-3): role in functionality and cell biology. Am J Physiol Cell Physiol 316:C805–C814
39. Hildebrandt F, Otto E (2000) Molecular genetics of nephronophthisis and medullary cystic kidney disease. J Am Soc Nephrol 11:1753–1761
40. Beitner-Johnson D, Ferguson T, Rust RT, Kobayashi S, Millhorn DE (2002) Calcium-dependent activation of Pyk2 by hypoxia. Cell Signal 14:133–137
41. Lu H, Chen I, Shimoda LA, Park Y, Zhang C, Tran L, Zhang H, Semenza GL (2017) Chemotherapy-induced Ca(2+) release stimulates breast cancer stem cell enrichment. Cell Rep 18:1946–1957